CHAPTER 3

Complexes of bis(oxamido) hydrazones with amino acids: Synthesis, characterization, Magnetism and Electrochemical studies.

3.1 Introduction

As said in chapter one, a number of metalloproteins and metalloenzymes are known to have binuclear or trinuclear active sites. Many others are shown to possess multimetal clusters. The enzyme tyrosinase contains a Type 3 i.e. coupled binuclear active site with an oxo-bridge and the histidine residues of the protein occupying other coordination positions. Dopamine-β-hydroxylase, which is a normal copper protein, contains four copper centres, a disulfide bridged dimer. Multinuclear blue copper oxidases - ceruloplasmin, ascorbic acid oxidase and laccase - are the enzymes which mediate four electron reduction of oxygen by substrates to water without releasing superoxide or peroxide as intermediates. This property is related to the presence, in the same protein molecule, of at least four copper ions, divided in to three spectroscopically distinguishable centres, which are referred to as the Type 1, or "blue" copper (with an intense optical absorption around 600nm and a very small A_{II} hyperfine splitting in the EPR spectrum.), Type 2, or "non-blue" or "normal" copper (with no apparent visible absorption and large A_{II} values), and Type 3 copper (absorbing at 300nm in the optical spectrum, and not detectable by EPR). The Type 3 copper is likely to be made up of two antiferromagnetically coupled copper(II) ions. The crystal structures of cytochrome c oxidase from bovine heart[1] and from the bacterium P. denitrificans[2] have recently been solved at 2.8Å resolution. The structures confirm that the Cu_A centre is binuclear and that the coppers are coordinated by Cys-196, Cys-200, His-161, His-204, Met-20, and the backbone carbonyl of Glu-198 (bovine numbering). The side chain carboxylate of Glu-198 lies buried at the interface between subunits I and II, far from the surface of the protein, and coordinates a magnesium(II) ion at the subunit interface. The magnesium(II) ion is located along a potential electron transfer path from Cu_A to the heme edge of cytochrome a_3. It is well known that an aminocarboxylate anion or its acid coordinates to a cobalt(III) ion as a unidentate,[3] or a bidentate,[4-8] and in some cases also as a tridentate ligand such as aspartate[9-10] and histidinate.[11]

All multicopper oxidases have varying combinations of Type 1, Type 2, and Type 3 active sites. A number of times two or more active sites combine with each other or work in concert to be effective as a trinuclear or a multinuclear

active centre e.g. the trinuclear active site in laccase and ascorbic acid oxidase are in fact combinations of Type 3 and Type 1 active sites linked with each other through a tripeptide, his-cys-his. Type 3 copper in these trinuclear active sites has a μ-oxo bridge with two histidine nitrogens bound to each copper. While the cysteine sulfur along with methionine sulfur and nitrogen of two more histidine residues form the coordination sphere of Type 1 copper. Presence of copper trinuclear clusters is found to be essential in mammalian ceruloplasmin for efficient electron transfer to oxygen. This is a trinuclear Type 2 - Type 3 cluster[12] undergoing reversible redox.

The nature of the amino acid bound to copper in the oxygenase enzymes has an important role, since they decide or manipulate the electronic environment around the active metal centre e.g. the presence of coordinated cysteine sulphur can stabilize copper(I) centre in an enzyme. The histidine nitrogens are relatively hard ligands as compared to cysteine sulphur yet they being a part of delocalized π-system or π-bonding in character can help a reversible redox of copper active site at higher potential than Type 1 copper. The environment in Type 2 or normal copper is usually a histidine, an aspartate, a glutamate and water. Typically, the coordination positions are occupied by non aromatic or ionic amino acids and σ-bonding amino acid residues. This coordination environment makes the active site behave as a normal square planar copper, which is easily reducible. The understanding of the redox potentials associated with each type of copper site in various enzymes guides the development of active site mimics as catalysts.

Bio-inspired catalytic oxidations by copper complexes mimicking enzyme active sites are intensively pursued in view of their potentially interesting synthetic applications.[13] Basically all studies reported so far focused on catalytic systems consisting of mono or dinuclear copper complexes which reproduce structural or functional features of enzyme centres of similar nuclearity, Type 2 or Type 3 copper, respectively.[14] Trinuclear complexes have been little investigated,[15] in-spite of the fact that clusters encompassing combinations of sites, e.g. Type 2 - Type 3 copper assembly, are contained in the well known groups of multicopper oxidases, in association with a mononuclear Type 1 copper site.[16] Amino acids in combination with ligands such as ethylenediamine, can

form stable trinuclear complexes with tin(IV) and copper/nickel(II). A literature survey reveals that the copper(II) ion binds to the guanine in the DNA helix while tin(IV) prefers to bind to the phosphate backbone of the DNA double helix.[17] The introduction of the chirality, due to the presence of L-tryptophan in the complex, enhances the selective binding of the complex to the target site.[18] The chiral auxiliary as tryptophan incorporated in the metal complexes can generate more selective and active metal centre, which is well tuned to adopt a different stereochemistry. The interaction studies of the described complex with calf-thymus DNA suggest that the complex is strong stereoselective inhibitor of DNA. This complex is proved to be a promising candidate for cancer chemotherapy.[19] Several proteins and peptides like gly-his-lys are efficient chelators of copper and they function to enhance the cellular uptake of copper under specific conditions. Affinity of these peptides of copper varies as the constituent amino acids.[20] A trinuclear copper complex of PHI, a trinucleating ligand containing chiral 'L-his' residue, has been derived from pyrimidine and two flexible arms containing, 1,4-diaminobutane derivatives. This coordinates copper centres bound to imidazoles. The complex is capable of catalytic oxidation of L- and D-dopa with remarkable enantiomeric differentiations. The CD spectral studies have shown that the complex Cu_3PHI can have stronger binding with various L-amino acids than the D-amino acids. Thus the complexes can also behave as enantioselective receptors for various amino acids.

Thus, it can be seen that, the amino acid environment around an active centre can affect the energy of participating molecular orbitals and thus modify its spectroscopic, chemical, redox and catalytic properties. It was thought of interest to incorporate various aromatic, hydrophilic and hydrophobic amino acids in the trinuclear complexes as non bridging ligands and see their effect on the energy of metal orbitals and hence on the magnetic exchange through relatively efficient oxamide bridges.

3.2 Experimental

Materials

AR quality ethyl oxamate, hydrazine hydrate and glyoxal were purchased from Merck. Methanol and DMSO used for electronic spectroscopy and cyclic

voltammetric studies, respectively, were of AR or spectroscopic grade and were purchased from Merck. Tetrabutyl ammonium perchlorate (TBAP) used in voltammetric studies was AR and obtained from Fluka. All reagents were used as received. All other solvents were distilled before use.

Synthesis of oxamido hydrazine, oxm (scheme-1)

1.600ml, (1.236g, 0.024mmol) of hydrazine hydrate was kept in a 100ml flask in 20ml of ethanol and allowed to reflux. An ethanolic solution of 1.080g (0.009mmol) of ethyl oxamate was added slowly, drop wise at reflux condition. During the addition, white crystalline product started separating. After complete addition, the reaction mixture was allowed to reflux under the same conditions for 5hrs. The product was filtered, washed thoroughly with ethanol and dried in air. The product gives a single spot on TLC with polar and non polar solvent phases. m. p. = 278°C.

Synthesis of trinucleating ligand oxmglx (L)

A solution of glyoxal, 0.500g (2.379mmol) in 10ml of ethanol, with 2-3 drops of glacial acetic acid was heated to reflux. A suspension of **oxm** (0.430g, 4.758mmol) in ethanol was added slowly to the above refluxing solution. After complete addition the reaction mixture was allowed to reflux overnight. The pure white colour of the **oxm** ligand, changed to off white and the spots of glyoxal and **oxm** on TLC disappeared completely. The product was filtered and washed severally with ethanol and dried in air. m.p. = 276°C. (dec)
Elemental Analysis observed: C = 31.24%, H = 3.69% and N = 37.38%: Calculated for the formula $C_6H_8O_4N_6$; C = 31.57%, H = 3.50% and N = 36.84% with yield = 53.16%.

Synthesis of Tri-nuclear complexes

Synthesis of trinuclear complex [oxmglxCu$_3$(anthr)$_2$](Ac)$_2$ (3.1)

0.200g (0.877mmol) of the trinucleating ligand, **oxmglx** and 0.272g (1.754mmol) of anthranilic acid (anthr) were mixed in a 100ml flat bottom flask in 30ml absolute ethanol. The suspension was allowed to reflux for 30min. 0.525g (0.877mmol) of cupric acetate monohydrate in 30ml absolute ethanol was added slowly drop wise within 15min under reflux condition.

Scheme-3.1

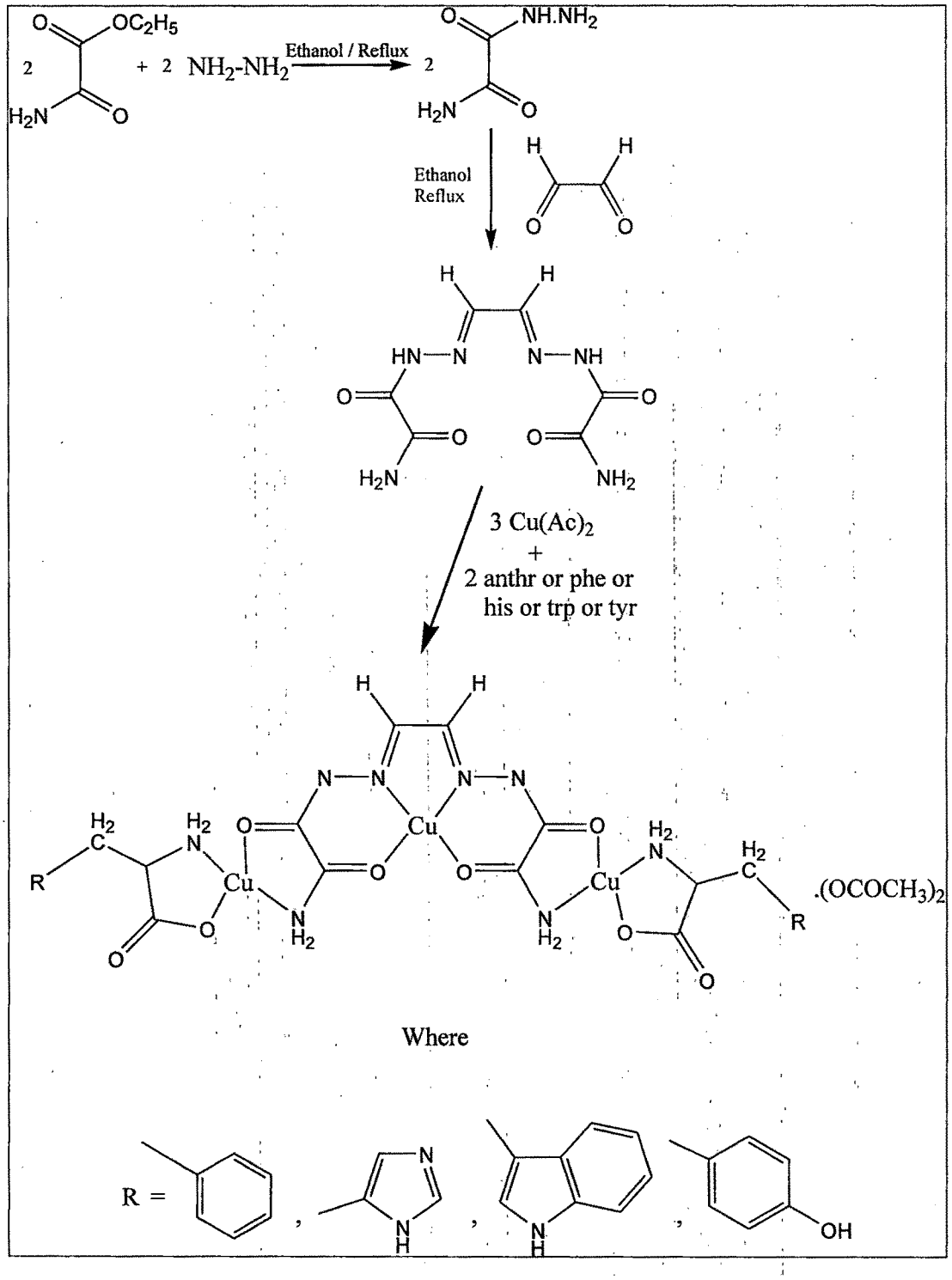
Ethanol / Reflux
Ethanol
Reflux
3 Cu(Ac)2
+
2 anthr or phe or
his or trp or tyr
.(OCOCH3)2
Where
R =

Two more portions of 0.525g (0.877mmol) of cupric acetate monohydrate in 30ml absolute ethanol were added slowly over duration of 15min. each after maintaining a gap of 5-10min. During the addition of cupric acetate monohydrate, the suspension of ligand started dissolving, and at the end of the addition, the solution became clear and dark green in colour. After half an hour, a green coloured microcrystalline complex started separating. The mixture was then held at the reflux condition for further 4.5hrs to ensure completion of the reaction. The product was filtered, washed thoroughly with ethanol and dried in air.

Synthesis of trinuclear complex [oxmglxCu$_3$(phe)$_2$](Ac)$_2$ (3.2)

0.200g (0.877mmol) of the trinucleating ligand, **oxmglx** was dissolved in 30ml absolute ethanol and was hearted to reflux. 0.525g (0.877mmol) of cupric acetate monohydrate in 30ml absolute ethanol was added slowly drop wise within 15min. under reflux condition. Separately, 0.289g (1.754mmol) of phenylalanine (phe) was mixed with 1.056g (1.754mmol) of cupric acetate monohydrate in 30ml absolute ethanol. This resulted in the formation of blue coloured [Cuphe]$^+$ complex. The suspension of [Cuphe]$^+$ complex was added to the above refluxing solution. During the addition of [Cuphe]$^+$ complex the solution became clear and the colour of the solution changed to dark green. After half an hour, a green coloured microcrystalline complex started separating. The mixture was then held at reflux condition for further 4.5hrs to ensure completion of the reaction. The product was filtered, washed thoroughly with ethanol and dried in air.

Other complexes in the series have been synthesized following the above procedure and using equivalent quantities of histidine **(3.3)**, tryptophan **(3.4)** and tyrosine **(3.5)** as secondary ligands in place of phenylalanine, respectively.

Physical Measurements

All the physical measurements, UV-vis, IR and ESR spectral analysis, FAB-Mass analysis and cyclic voltammetric studies were carried out using the instruments as mentioned earlier in chapter 2 (page no.79).

Table 3.1: Yields and analytical data of the ternary complexes of **oxmglx**

Complex	Yield (%)	Elemental Analysis (%)		
		C	H	N
[oxmglxCu$_3$(anthr)$_2$](Ac)$_2$ $C_{24}H_{24}O_{12}N_8Cu_3$	84.86	35.81 (35.70)	3.39 (2.97)	14.22 (13.88)
[oxmglxCu$_3$(phe)$_2$](Ac)$_2$ $C_{28}H_{38}O_{15}N_8Cu_3$	68.71	36.25 (36.65)	3.99 (4.14)	12.69 (12.21)
[oxmglxCu$_3$(his)$_2$](Ac)$_2$ $C_{22}H_{32}O_{12}N_{12}Cu_3$	79.99	31.61 (31.18)	4.20 (3.77)	19.67 (19.84)
[oxmglxCu$_3$(trp)$_2$](Ac)$_2$ $C_{32}H_{34}O_{12}N_{10}Cu_3$	81.48	40.82 (40.82)	3.95 (3.61)	14.52 (14.88)
[oxmglxCu$_3$(tyr)$_2$](Ac)$_2$ $C_{28}H_{32}O_{14}N_8Cu_3$	47.55	37.12 (37.55)	3.84 (3.57)	12.67 (12.51)

3.3 Results and Discussion

Characterization of oxmglx ligand

The elemental analysis of newly synthesized bis-oxalodiamide ligand was found within the appreciable range. In the IR spectrum of the ligand **oxmglx**, the band corresponding to >C=O stretching in amide has been observed at 1659cm^{-1}. The $\nu_{>C=N}$ vibration remains merged with the former, making it broad. The N-H strechings corresponding to the primary and secondary amide groups have been observed at 3227 and 3383cm^{-1}, while the bending in the primary amide has been observed at 1602cm^{-1}. The –C-N- stretching and bending (amide) has been observed at 1413, 1122, 1160 and 1063cm^{-1}.

In the ^{1}H NMR spectrum of the complex recorded in DMSO solution, two singlets corresponding to both the $-NH_2$ were observed at 5.9 and 6.2ppm. A singlet corresponding to –N=C-H (a) was observed at 7ppm and another singlet corresponding to –NH was observed at 7.9ppm. Splitting of both the $-NH_2$ protons was also supported by the theoretical studies of the ligands and further discussed in the next part. These values in ^{1}H NMR spectrum support the formation of the trinucleating ligand, **oxmglx**, with the suggested structural formula

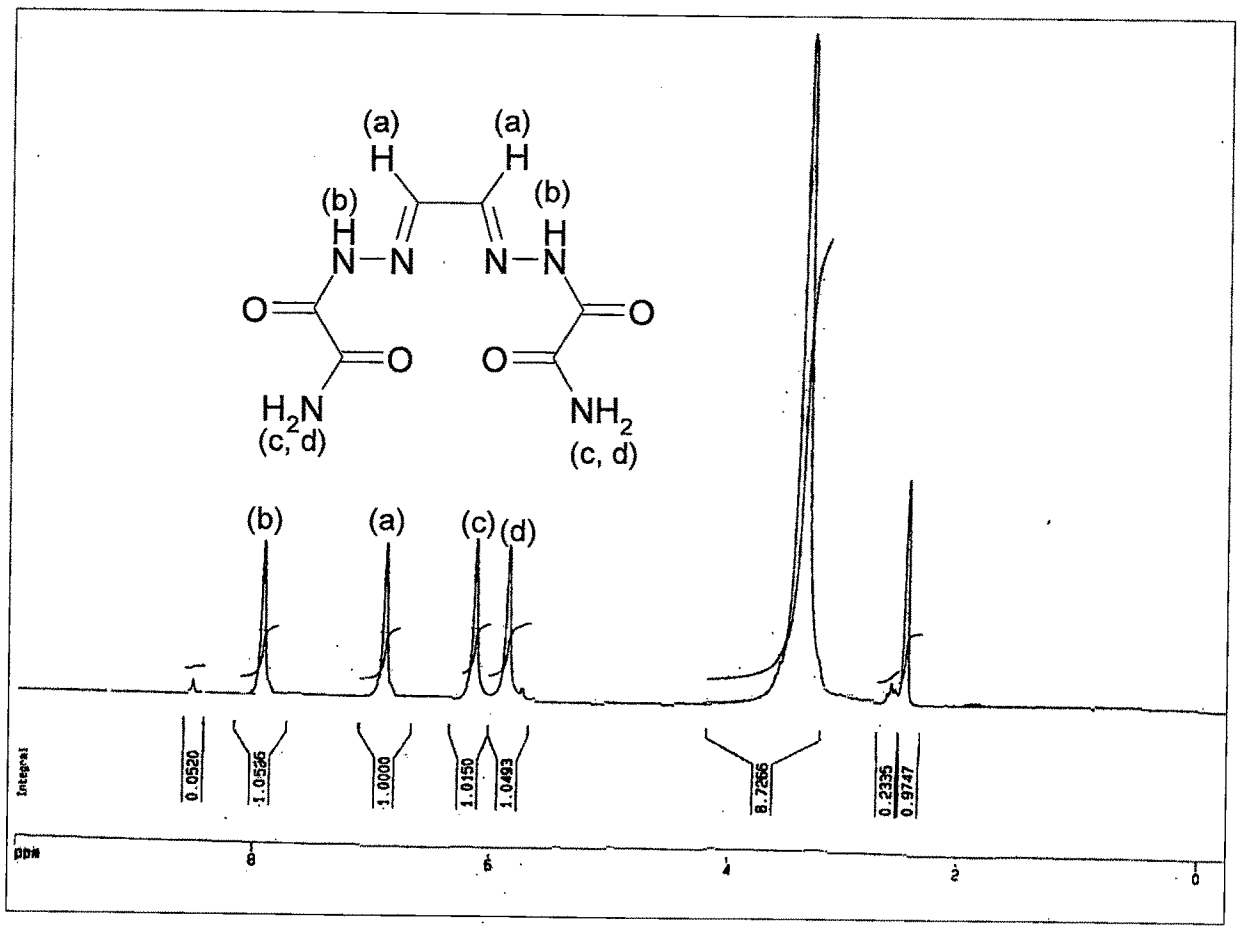

Fig.3.1 ^{1}H NMR spectrum of ligand **oxmglx.**

Characterization of the Complexes

All five complexes were obtained in good yields. The elemental analyses of the complexes agree with the suggested formulae. Because of the poor solubility of complexes in suitable solvents, molar conductivity values could not be accurately measured.

FAB Mass spectra of complexes

Of the five complexes, **[oxmglxCu$_3$(trp)$_2$](Ac)$_2$** (**Fig.3.5**) has appreciable solubility in m-nitrobenzyl alcohol. FAB-Mass spectrum of this complex along with that of **[oxmglxCu$_3$(his)$_2$](Ac)$_2$**, (**Fig.3.3**) and **[oxmglxCu$_3$(tyr)$_2$](Ac)$_2$** (**Fig.3.7**) were recorded. Some of the important fragements of the complexes are listed below, in **Fig.3.2**, **3.4** and **3.6** and in the Table. 3.2 to 3.4.

In the mass spectrum of the complex, **[oxmglxCu$_3$(his)$_2$](Ac)$_2$**, the peak at m/Z=785 is a prominent peak and corresponds to the mono cation **[oxmglxCu$_3$(his)$_2$]Ac$^+$** (**Fig.3.3**). Other significant fragments include the complex with parent ligands and the binuclear complex left behind after dissociation of [Cuhis] unit at m/Z = 490. The mass spectrum also shows the formation of copper clusters.

Table 3.2 Important fragments of the complex **[oxmglxCu$_3$(his)$_2$](Ac)$_2$**

Description of species	Cal. (m/Z)	Obs. (m/Z)
Hhis+H$^+$	156	156
[Cuhis]$^+$	216	214
[Cuoxmglx]$^+$	289	289
[Cuoxmglx]H$_2$O$^+$	307	307
[oxmglxCu$_3$(his)$_2$](Ac)$^+$	782.54	785
[Cu$_2$oxmglxhis]$^+$	490	491
[Cu$_2$oxmglx]Ac$^+$	411	412
[Cu(his)$_2$]+H$^+$	375	376

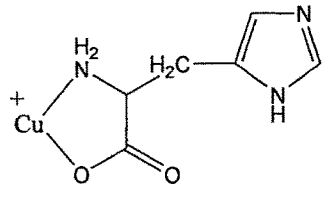

[Cuhis]$^+$ observed m/Z = 214 (216)

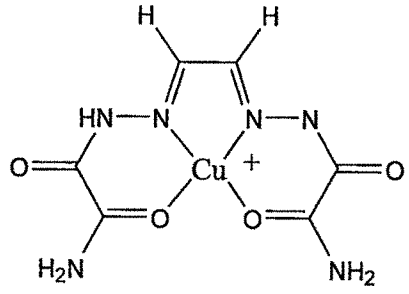

observed at m/Z = 289.

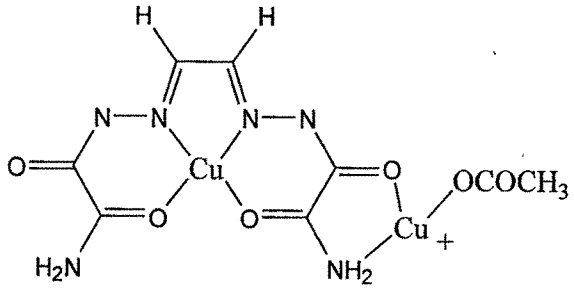

observed at m/Z = 412.

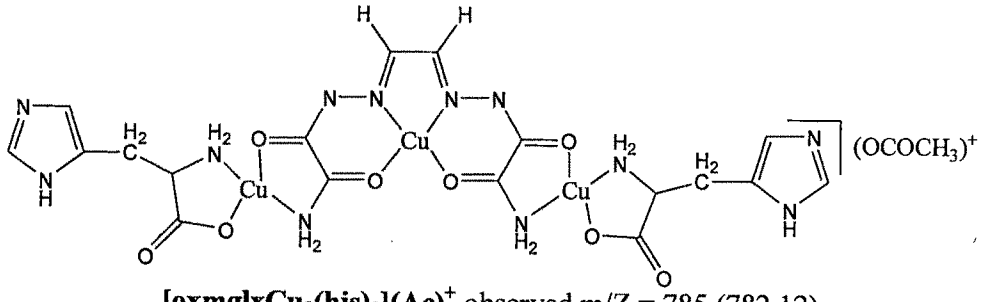

[oxmglxCu$_3$(his)$_2$](Ac)$^+$ observed m/Z = 785 (782.12)

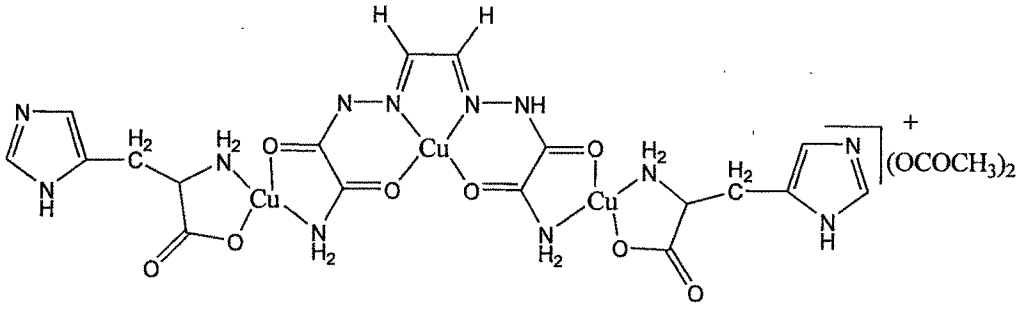

[HoxmglxCu$_3$(his)$_2$](Ac)$_2^+$ observed m/Z = 842 (842.12)

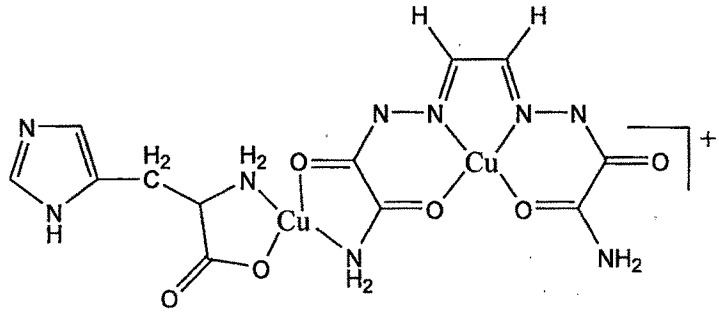

$[Cu_2oxmglxhis]^+$ observed m/Z = 490 (491)

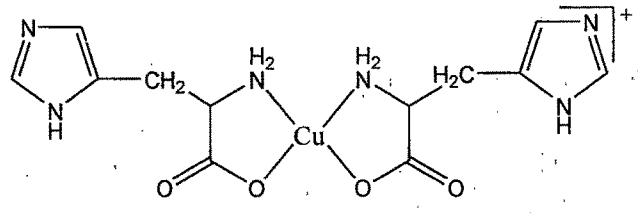

$[Cu(his)_2]+H^+$ observed m/Z = 376 (376)

Fig.3.2

In the mass spectrum of **$[oxmglxCu_3(trp)_2](Ac)_2$ (Fig.3.5)**, the molecular ion peaks $M+H^+$, $M+2H^+/2$ i.e. **$[oxmglxCu_3(trp)_2](Ac)_2+H^+$** and **$[oxmglxCu_3(trp)_2](Ac)_2+2H^+/2$** are prominently observed at m/Z = 940 and 470, respectively. The complex species, with one acetate and without acetate have very low abundance. The reduced complex ion peak **$[oxmglxCu_3(trp)_2]^{2+}-H^+$** has been observed with low abundance with m/Z = 821. The species corresponding to the loss of trp and $[Cutrp]^+$ are observed with low abundance at m/Z = 618 and 555, respectively. The copper clusters formed by the trinuclear complexes by association with one and two copper ions have also been observed at m/Z 1004 and 1069, respectively.

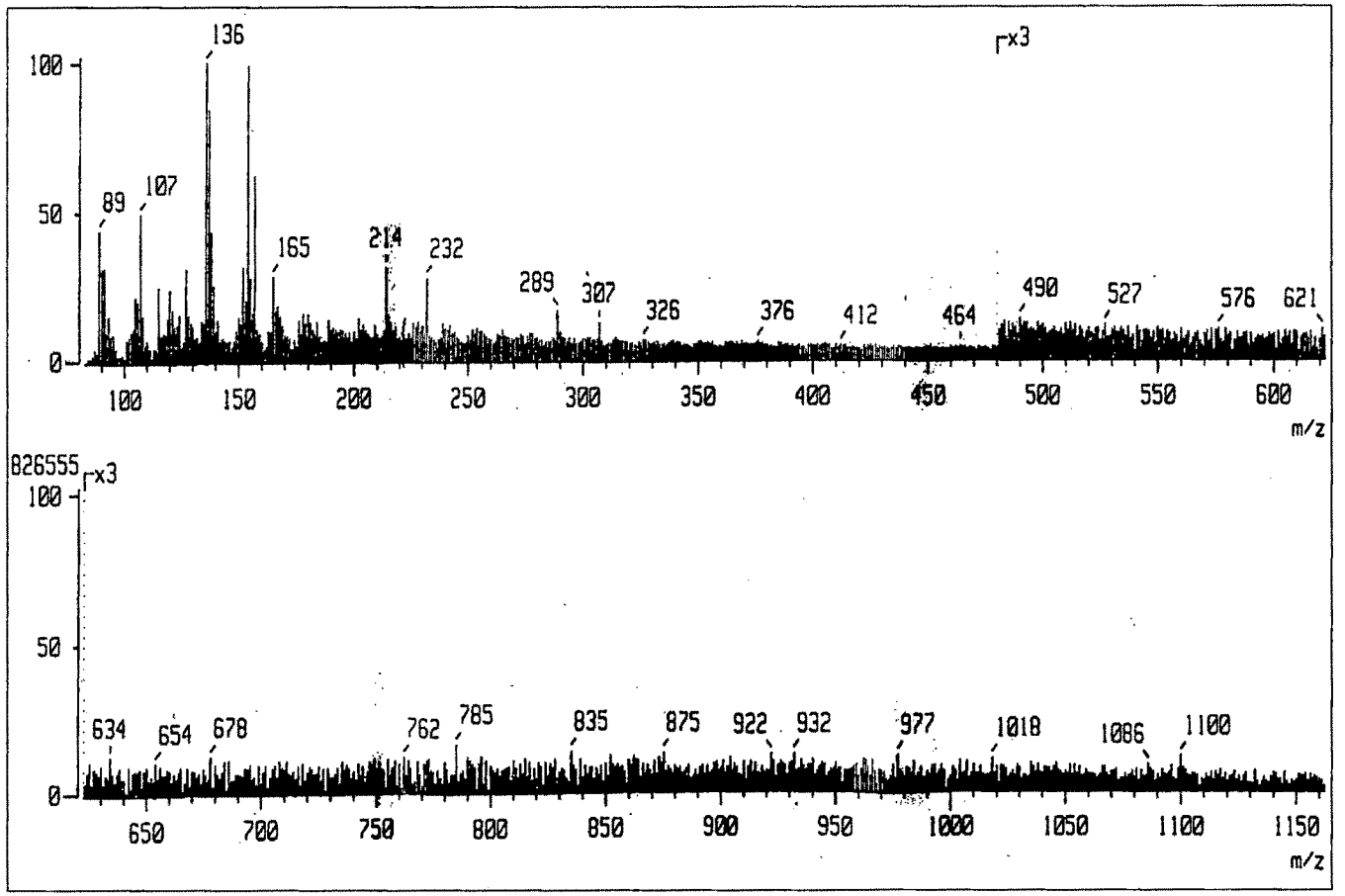

Fig.3.3 FAB-Mass spectrum of Complex **[oxmglxCu$_3$(his)$_2$](Ac)$_2$.**

Table 3.3 Important fragments of the complex **$[oxmglxCu_3(trp)_2](Ac)_2$**

Description of species	Cal. (m/Z)	Obs. (m/Z)
$[Cutrp]^+$	267	267
$[oxmglxCu_3(trp)_2](Ac)_2+2H^+/2$	470.56	470
$[Cu_2oxmglx](Ac)_2^+$	470	470
$[Cu_3oxmglx](Ac)_2^{2+}$	533	533
$[Cutr(C_4H_5O_2N_3)]^+$	396	396
$[oxmglxCu_3(trp)_2](Ac)_2+H^+$	940	942
$[Cuoxmglx]+H^+$	289.54	289
$[Cu_2trp(C_2H_4O_2N_3](Ac)_2^+$	548	548
$[Cuoxmglx]H_2O^+$	307	307
$[Cu_2oxmglx]Ac^+$	411	412
$[Htrp]+H^+$	204	204
$[oxmglxCu_3(trp)_2](Ac)+Cu$	1003	1004

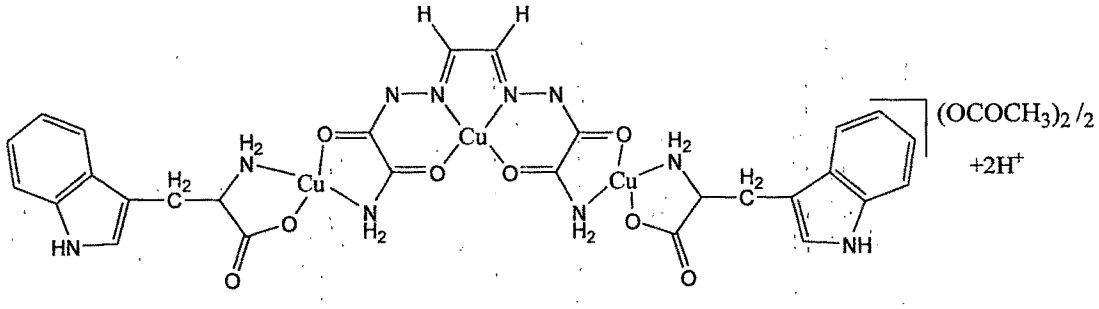

$[oxmglxCu_3(trp)_2](Ac)^{2+}/2$ observed m/Z = 470 (470)

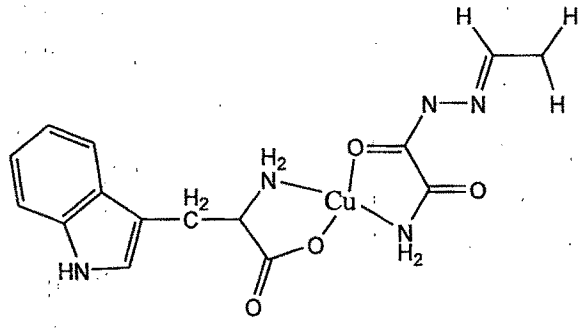

observed m/Z = 396 (396)

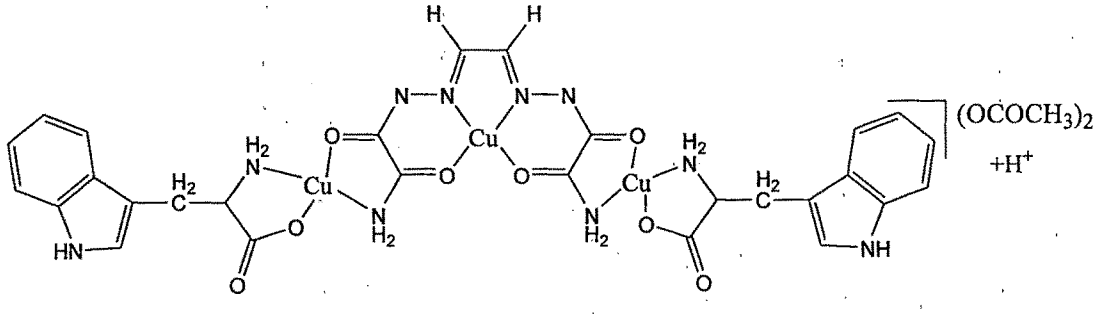

$[oxmglxCu_3(trp)_2](Ac)^{2+}$ observed m/Z = 940 (940.12)

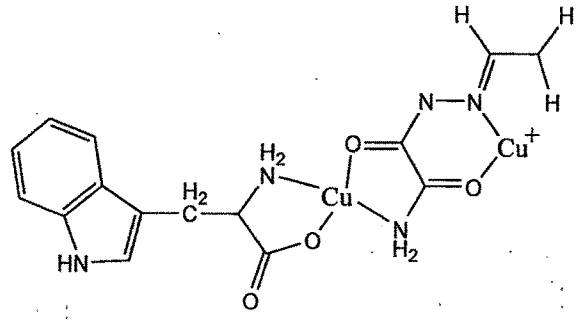

observed m/Z = 459 (459)

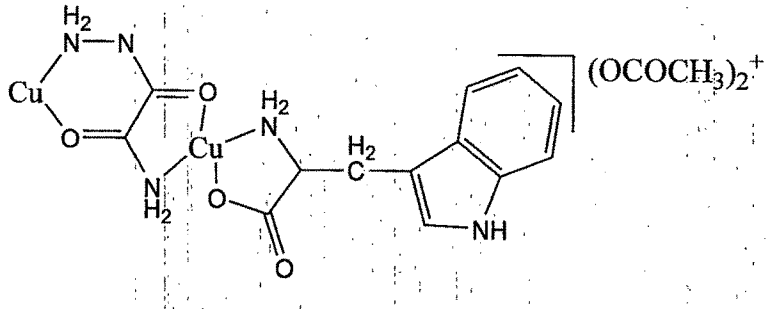

observed m/Z = 548 (548)

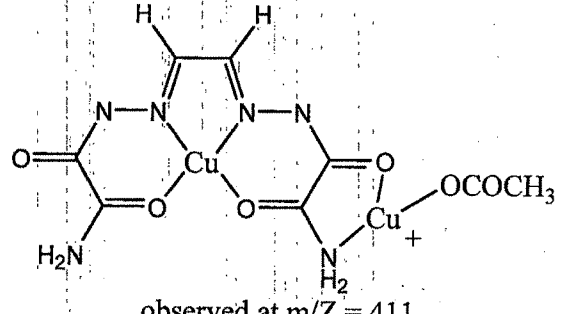

observed at m/Z = 411.

Fig.3.4

The quality of mass spectrum of **[oxmglxCu$_3$(tyr)$_2$](Ac)$_2$ (Fig.3.7)** is also poor due to very low solubility of the complex. Yet some of the important fragments could be identified including the molecular ion peak i.e. **[oxmglxCu$_3$(tyr)$_2$]$^{2+}$/2** at m/Z = 391, **[oxmglxCu$_3$(tyr)$_2$](Ac)$_2$+H$^+$** at m/Z = 895. The peaks observed at higher m/Z values 1038, 1085 and 1143 correspond to the copper clusters formed by the complex ions.

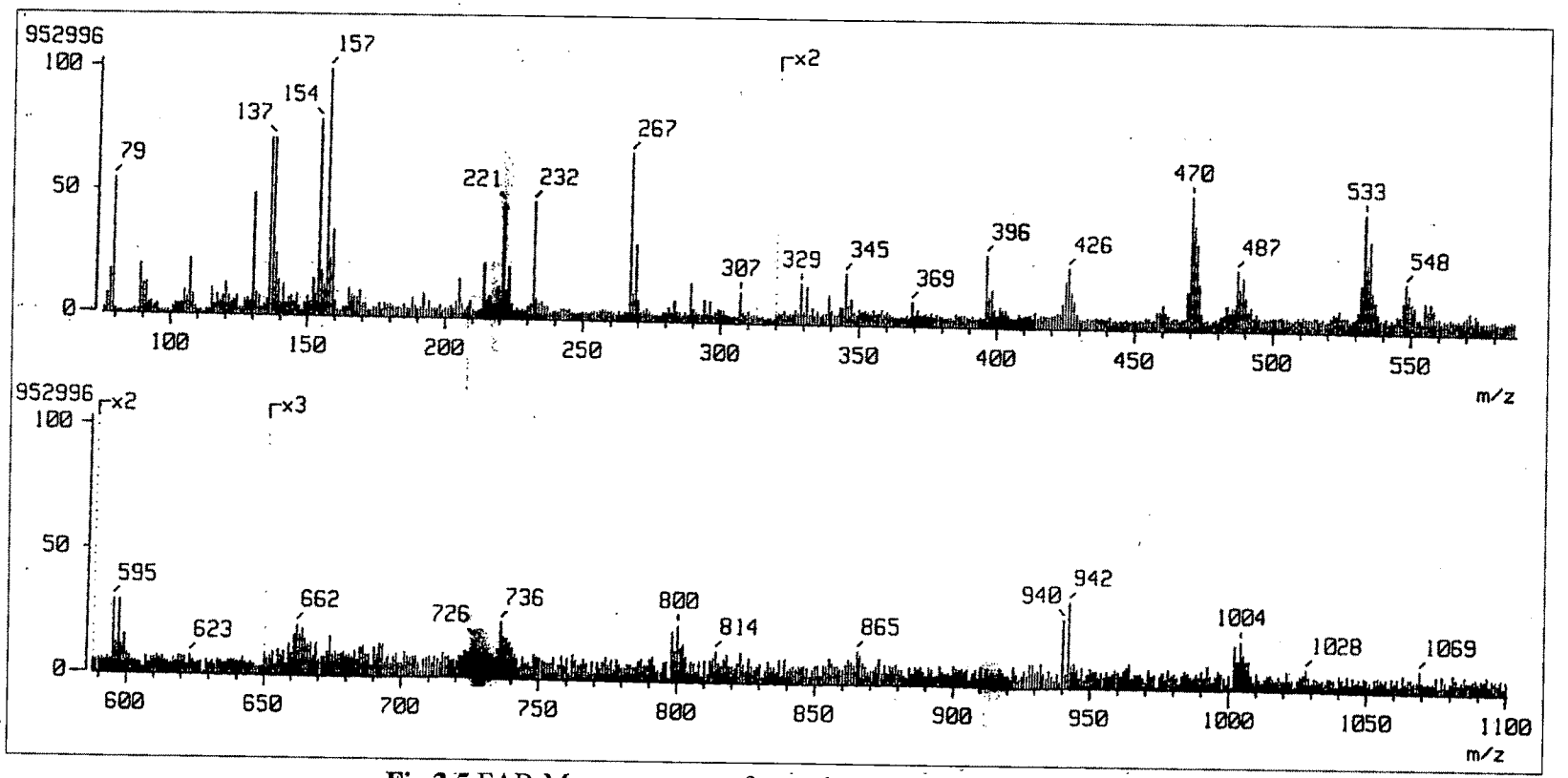

Fig.3.5 FAB-Mass spectrum of complex **[oxmglxCu$_3$(trp)$_2$](Ac)$_2$.**

Table 3.4 Important fragments of the complex **[oxmCu$_3$(tyr)$_2$](OCOCH$_3$)$_2$**

Description of species	**Cal. (m/Z)**	**Obs. (m/Z)**
[tyr+H$^+$]	181	181
[Cuoxmglx]$^+$	289	289
[Cuoxmglx]H$_2$O$^+$	307	307
[Cutyr]$^+$	243	244
[Cu$_3$(tyr)$_2$oxmglx](Ac)$^+$	834.12	834
[Cu(tyr)$_2$]$^+$	423	424
[oxmglxCu$_3$(tyr)](Ac)$_2$+H$^+$/2	447.5	447

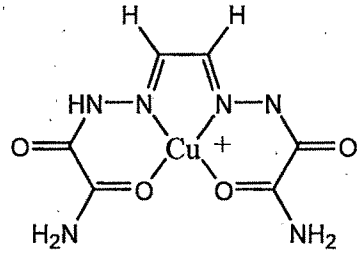

[Cuoxmglx] observed at m/Z = 289.

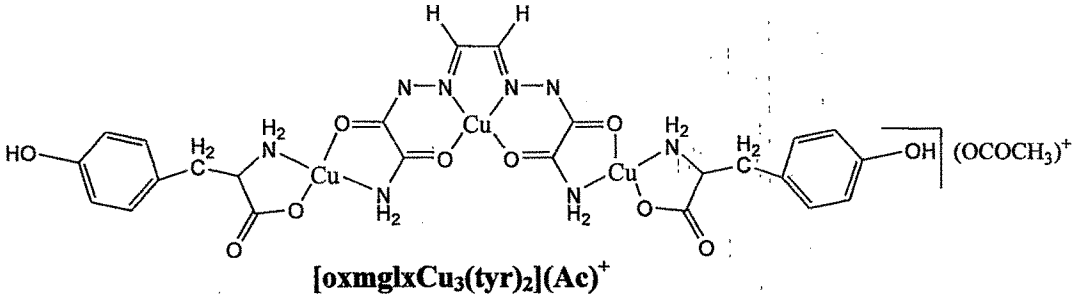

[oxmglxCu$_3$(tyr)$_2$](Ac)$^+$
Observed m/Z = 834 (834.12)

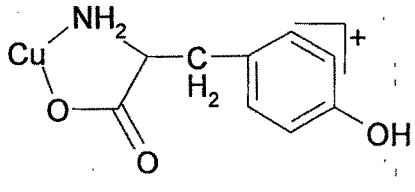

[Cutyr]$^+$ at m/Z = 244

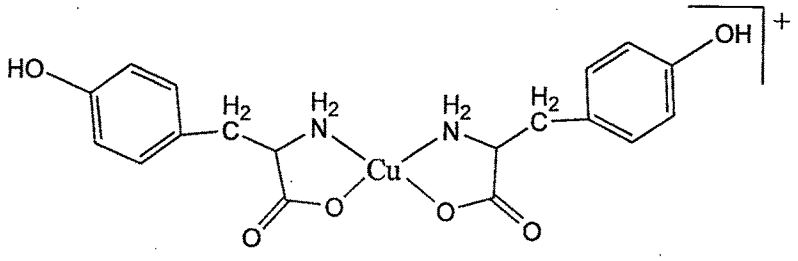

at m/Z = 424 $[Cu(tyr)_2]^+$

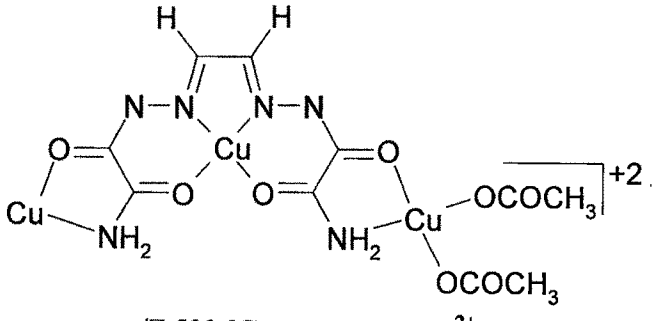

at m/Z 533 $[Cu_3oxmglx](Ac)_2^{2+}$

Fig.3.6

The observed Mass spectrum and corresponding important fragments described above support and confirm the formation of trinuclear complexes as per the suggested formulae.

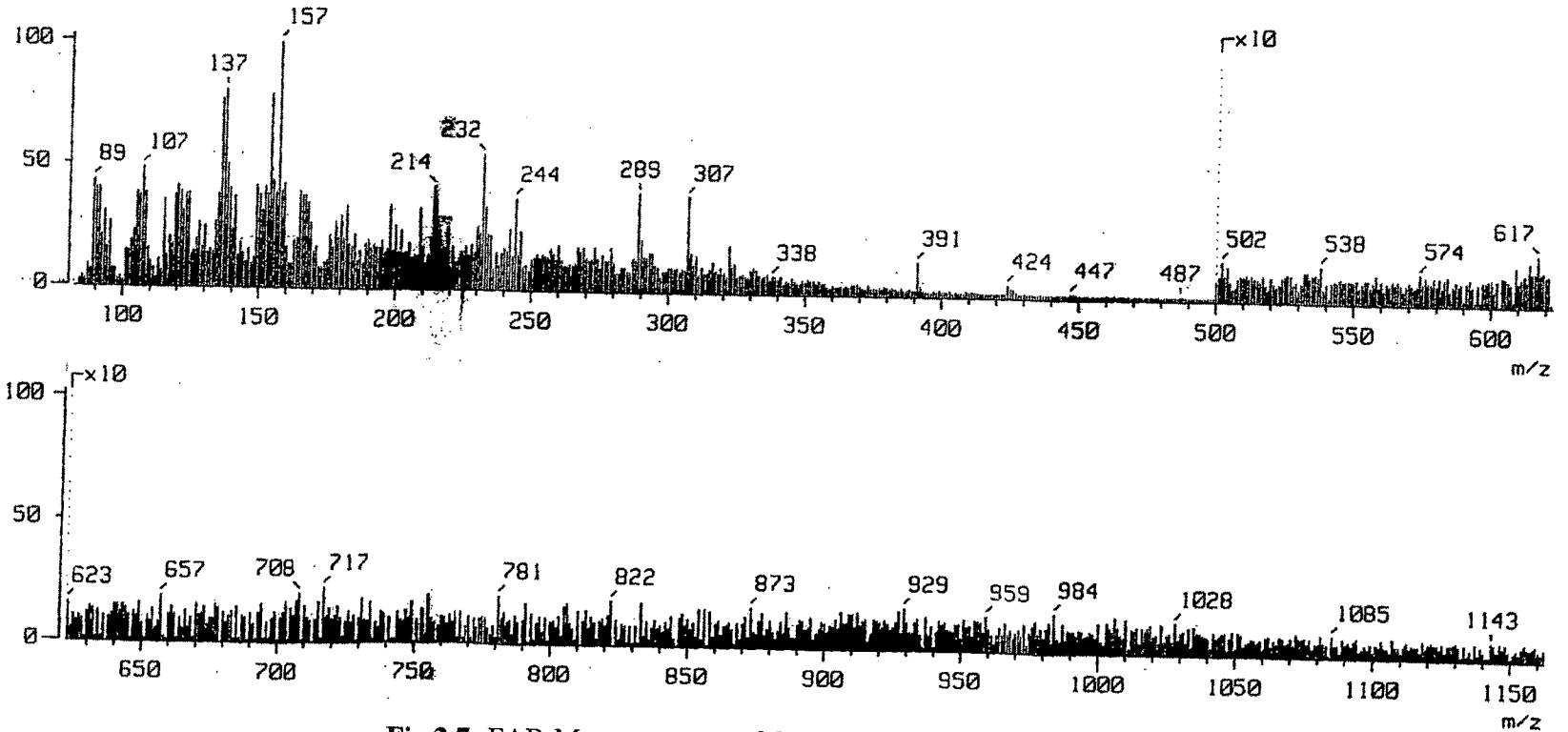

Fig.3.7 FAB-Mass spectrum of Complex **[oxmglxCu$_3$(tyr)$_2$](Ac)$_2$**

Electronic Spectra and FTIR spectral studies

The solubility of all complexes in noncoordinating solvents is very less. Hence, the electronic spectra were recorded using the saturated solutions in methanol. Ligand field transitions were not observed in all the complexes. The intra-ligand transitions were found to be present between 204 to 252nm in all the complexes. However, the ligand field transitions could not be seen.

In the trinuclear complexes of bis(oxalodiamide) unlike the ligand **oxmglx**, the –C=O- and –C=N- stretching frequencies are well separated. The –C=O stretching are observed at 1655, 1662, 1654, 1650 and 1657cm^{-1} in the complexes containing anthr, phe, his, trp and tyr, respectively. The >C=N- stretching has been observed in these complexes at 1606, 1621, 1632, 1625 and 1582cm^{-1}, respectively. Lowering in the $\nu_{-C=N-}$ confirm the involvement of imine nitrogen in the coordination with copper(II).

Table 3.5 Electronic absorption of complexes.

Complex	Intra ligand Transitions (nm)	Ligand Field Transitions (nm)
[oxmCu$_3$(anthr)$_2$](Ac)$_2$	204,252	Not Observed
[oxmCu$_3$(phe)$_2$](Ac)$_2$	209,214,241	Not Observed
[oxmCu$_3$(his)$_2$](Ac)$_2$	213	Not Observed
[oxmCu$_3$(tph)$_2$](Ac)$_2$	221	Not Observed
[oxmCu$_3$(tyr)$_2$](Ac)$_2$	209,218,227	Not Observed

Usually there is a metal to ligand π-interaction with imine nitrogen which lowers the strength of >C=N- and hence lowers the corresponding stretching frequency. The –N-H stretching has observed in the complexes between 3226 to 3390cm^{-1} as listed in Table 3.6. The –N-H bending in the primary amide is observed at 1552, 1529, 1587, 1580 and 1582cm^{-1}, respectively. Theses are shifted to lower frequencies as compared to the same vibrations in the free ligand. This is because of the extensive delocalization of nitrogen electron density through resonance on the amide oxygen which in terns donates electrons to copper(II) forming O→Cu coordinate bond. The lowering in –N-H bending is a conformation of this

resonance and coordination of amide oxygen with metal. Besides the vibrations in **oxmglx**, the IR spectra of the complexes also contain the bands corresponding to the –C-H- bending in aromatic ring in the amino acids between 742 to 760 and 680 to 700cm^{-1}. Also, absorption corresponding to –C=N- and carboxylate in coordinated amino acids are observed. In general the IR spectra are supportive of the suggested structures of the complexes.

The major and important frequencies are tabulated below.

Table 3.6 FTIR comparison of ligand and complexes.

Ligand (cm^{-1})		Complex (cm^{-1})				
Major Frequencies		**3.1**	**3.2**	**3.3**	**3.4**	**3.5**
>C=O	1659	1655	1662	1654	1650	1657
δN-H (bend)1^0	1602	1552	1552	1546	Merged	1582
δ N-H (bend)2^0	1531	1528	1529	Merged	Merged	1515
>C-N- (vibn) (Aliphatic)	1413,1180 1122,1063	1387,1152 1113,1063	1396, 1120,1063	1144, 1113, 1087	1152, 1111	1404, 1213, 1172, 1158, 1118, 1079, 1094,1057,
C-H (bend) Arm	------	756	699, 755	-------	695, 740	682, 769
C-H (bend) Alp	1307	1230	1229	1248	1228	
>C=N-	Merged with >C=O	1606	1621	1632	1625	----------
-NH_2	3227, 3383	3226, 3275,3378	3227, 3377	3230, 3382	3271, 3336, 3390	3160, 3309
Carboxylate Anion Stretching.	------	1387	1306, 1396	1325, 1343	1314, 1352, 1387	1307.1328, 1352

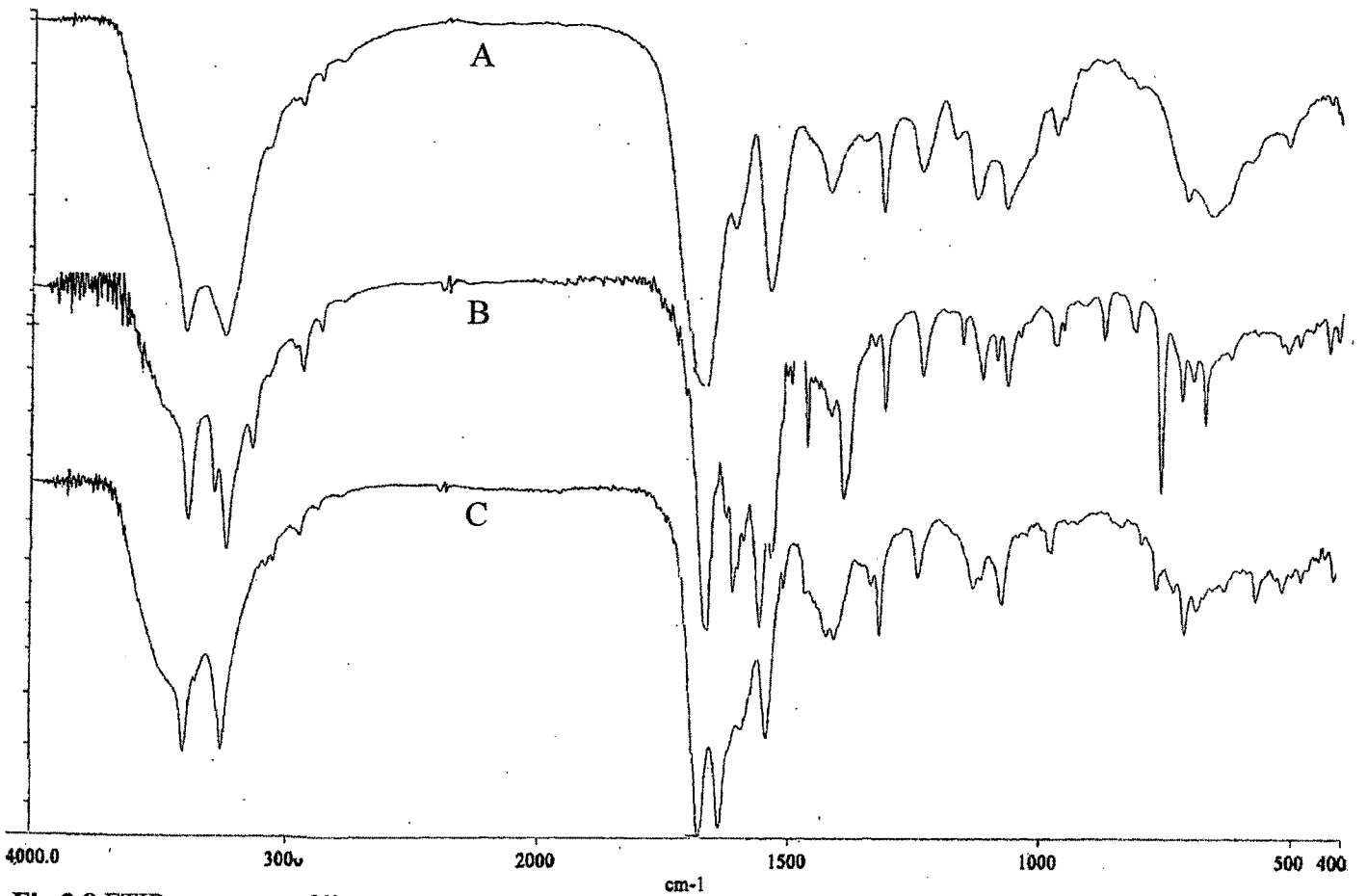

Fig.3.8 FTIR spectrum of ligand **oxmglx**, (A), **[oxmglxCu$_3$(anthr)$_2$](Ac)$_2$** (B) and **[oxmglxCu$_3$(phe)$_2$](Ac)$_2$** (C).

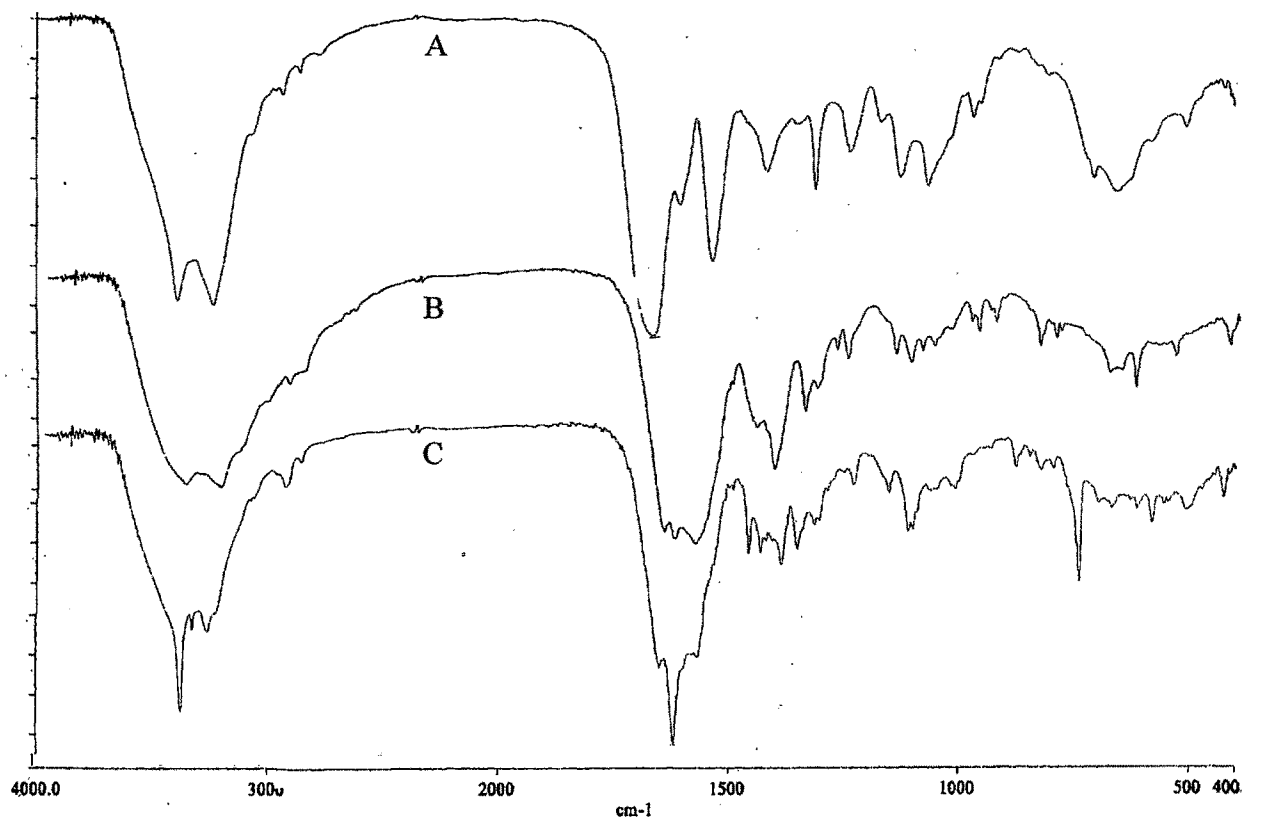

Fig.3.9 FTIR spectrum of ligand **oxmglx** (a) and the complexes **[oxmglxCu$_3$(his)$_2$](Ac)$_2$** (b) and **[oxmglxCu$_3$(trp)$_2$](Ac)$_2$ (c).**

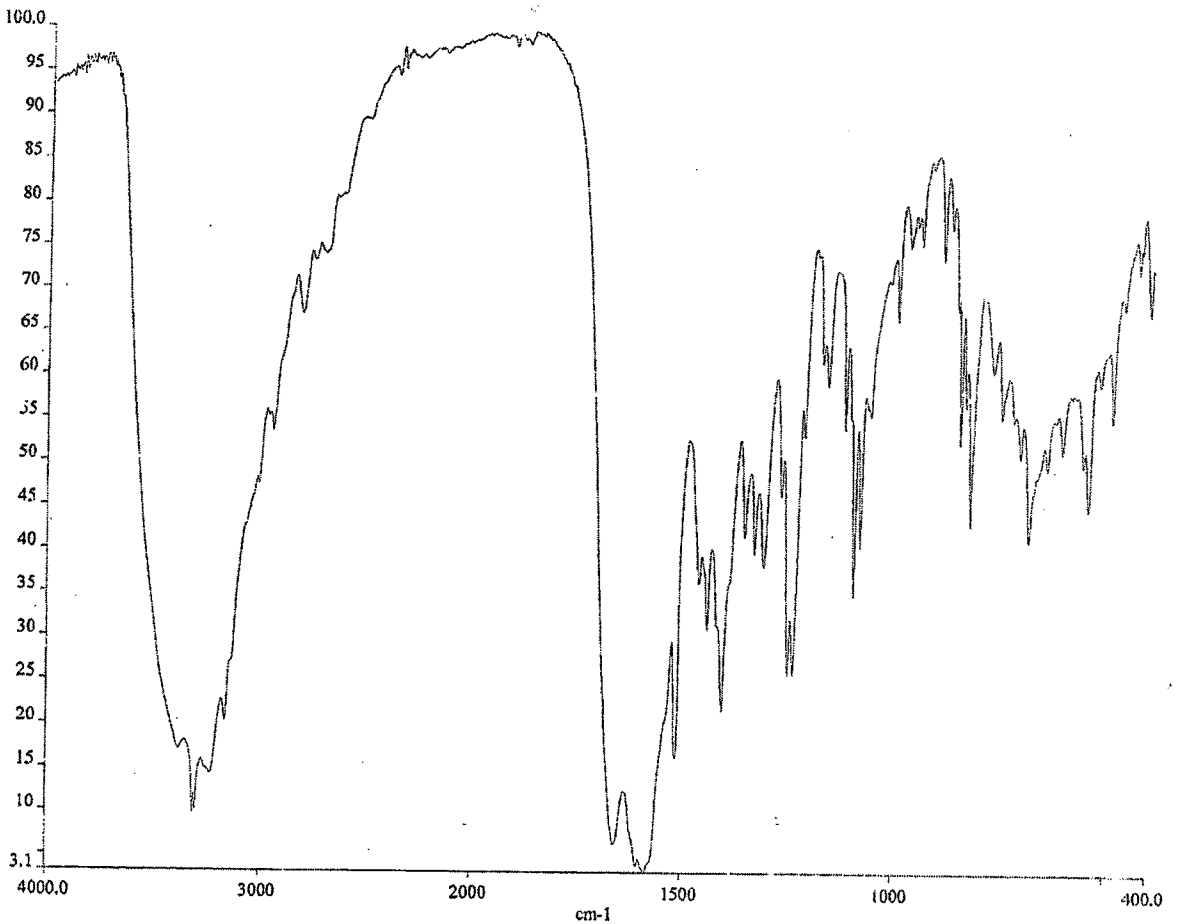

Fig. 3.10 FTIR spectrum of complex **[oxmglxCu$_3$(tyr)$_2$](Ac)$_2$.**

3.4 Molecular modelling

Ab initio quantum mechanical calculations[21] have been performed on the trinucleating ligand **oxmglx** using 6-31G basis set.[22-24] The calculation gives a very striking result with the lowest energy structure of the ligand and complexes having continuous delocalization of π-electron density.

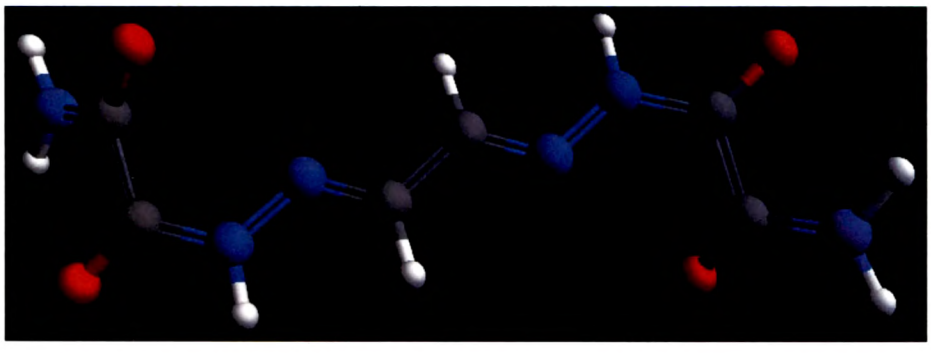

Fig.3.11 Structure of optimized ligand **oxmglx** by 6-31G basis set.

The –N-H bond distance corresponding to the two $-NH_2$ protons (primary amide) is observed to be different. One of the –N-H bond distances is 1.224Å where as the other is 1.219Å. This is because the hydrogen towards the neighbouring amide oxygen is hydrogen bonded and hence has longer –N-H bond distance. The presence of hydrogen bond formation supported by a shorter distance between this weakly bonded –N-H hydrogen and the adjacent amide oxygen, which is equal to 1.265Å. The same hydrogen bonded proton is found to be highly deshielded in the ^{1}H NMR of the ligand. The -C-C-, -C-N- and >C=O bond distances are all between the normal values of double and single bond distances between these atoms. This is result of extensive π-delocalization. The structure of the complexes with three heavy atoms and total of more than seventy is atoms far difficult for geometry optimization by *ab intio* methods or DFT.

In order to evaluate geometrical parameters related to the metal coordination planes and tortional angles. The molecular geometries have been optimized using Universal Force Field methods.[25-33] In the complexes the terminal copper centres have been found to be separated in space at a distance of 5.14 to 5.17Å. The distance between the neighbouring copper ions has been found to be 2.56 to 2.58Å. The copper ions are found to have angular arrangement with an angle of 165-170°. The dihedral angles between the metal coordination planes have been calculated (Table 3.7) and have been correlated with the values of exchange coupling constant J.

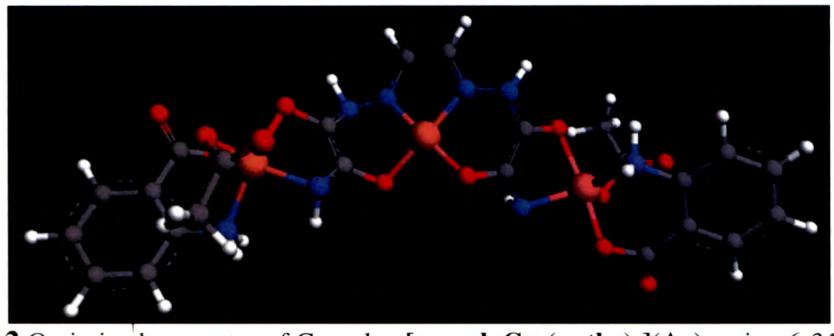

Fig. 3.12 Optimized geometry of Complex **[oxmglxCu$_3$(anthr)$_2$](Ac)$_2$** using 6-31 G basis set.

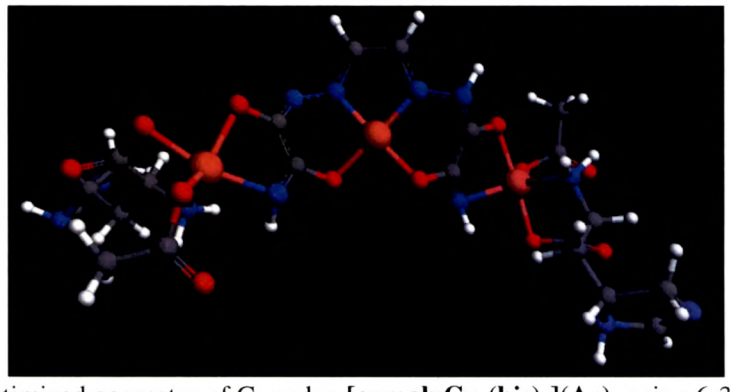

Fig. 3.13 Optimized geometry of Complex **[oxmglxCu$_3$(his)$_2$](Ac)$_2$** using 6-31 G basis set.

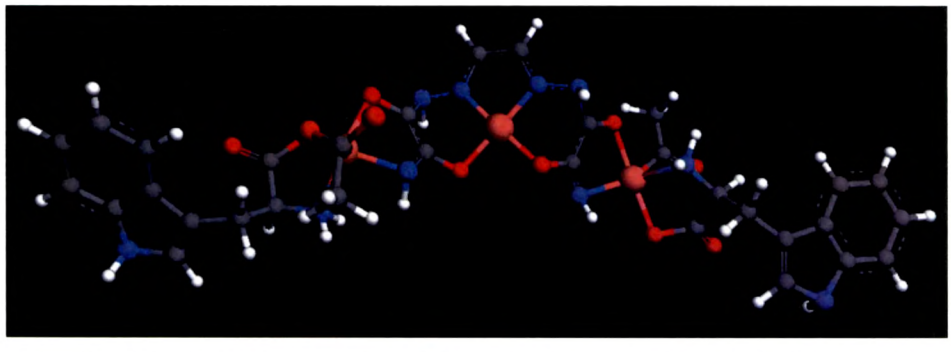

Fig. 3.14 Optimized geometry of Complex **[oxmglxCu$_3$(trp)$_2$](Ac)$_2$** using 6-31G basis set.

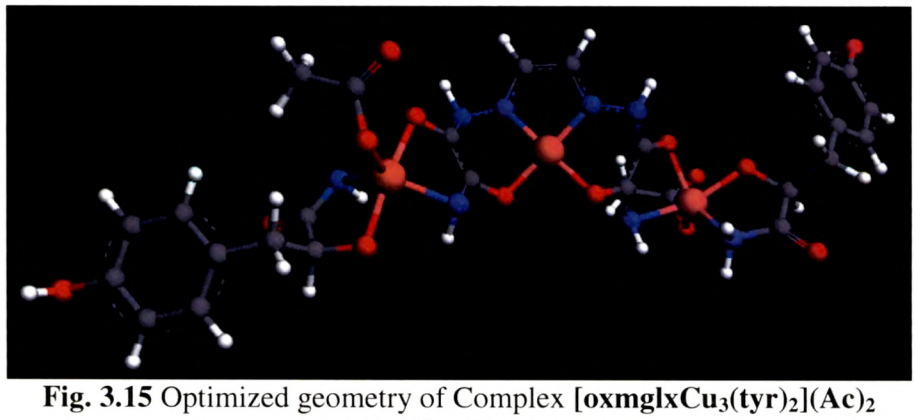

Fig. 3.15 Optimized geometry of Complex **[oxmglxCu$_3$(tyr)$_2$](Ac)$_2$** using 6-31 G basis set.

3.5 Magnetic properties of complexes

Plots of χ_M and μ vs T are shown in **Fig.3.16** to **3.19**.

Magnetic susceptibility of complexes **[oxmglxCu$_3$(anthr)$_2$](Ac)$_2$**, **[oxmglxCu$_3$(his)$_2$](Ac)$_2$**, **[oxmCu$_3$(trp)$_2$](Ac)$_2$** and **[oxmglxCu$_3$(tyr)$_2$](Ac)$_2$** was measured by Faraday method down to liquid nitrogen temperature.

Representative graphs of χ_M and μ versus temperature are shown in **Fig.3.16**,**Fig.3.17**, **Fig.3.18** and **Fig.3.19**.

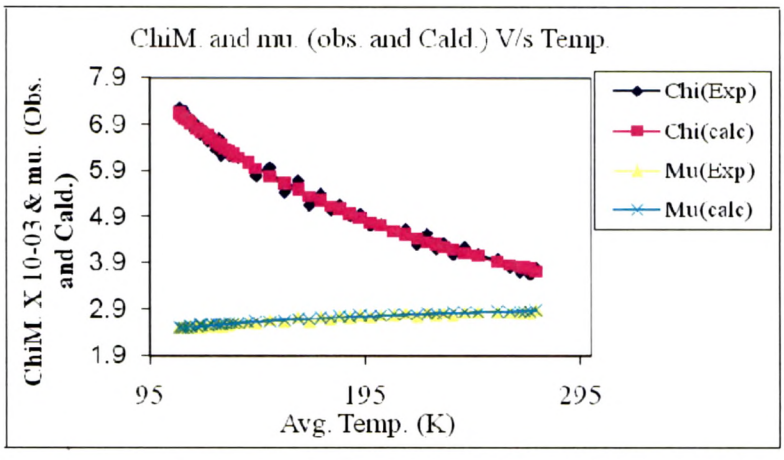

Fig 3.16 χ_M and μ (obsd. and calc.) v/s Temp. in **[oxmglxCu$_3$(anthr)$_2$](Ac)$_2$.**

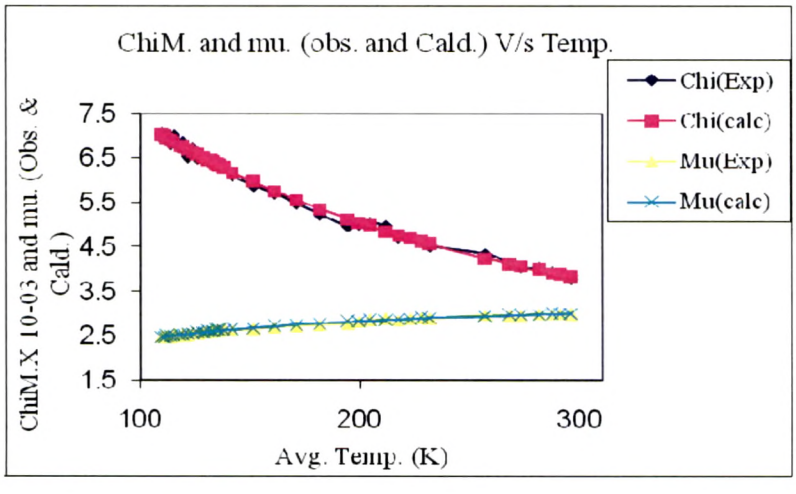

Fig. 3.17 χ_M and μ (obsd. and calc.) v/s Temp. in **[oxmglxCu$_3$(his)$_2$](Ac)$_2$.**

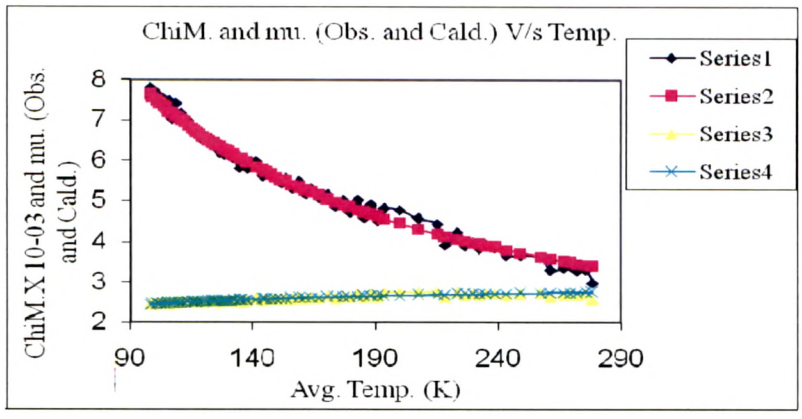

Fig. 3.18 χ_M and μ (obsd. and calc.) v/s Temp. in **[oxmglxCu$_3$(trp)$_2$](Ac)$_2$.**

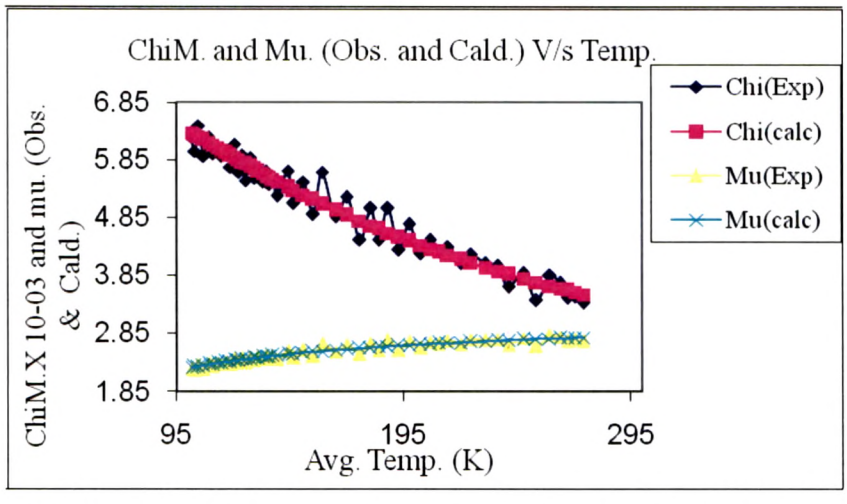

Fig. 3.19 χ_M and μ (obsd. and calc.) v/s Temp. in **[oxmglxCu$_3$(tyr)$_2$](Ac)$_2$.**

The complexes are found to be overall antiferromagnetic in nature. The values of exchange coupling constants J_1 between the terminal copper(II) centres and coupling constant J_2 between the neighbouring copper(II) ions are both found to be negative. The interaction between the two terminal copper(II) centres through the intervening and the bridging ligands is weakly antiferromagnetic with the values of J_1 ranging between -5 to -70cm^{-1}, while the interaction between the neighbouring copper(II) centres is strongly antiferromagnetic with J_2 equal to -100 to -250cm^{-1}.

Table 3.7 Values of Magnetic exchange parameters.

Complexes	Theta	J (cm^{-1})	Dihedral Angle
[oxmglxCu$_3$(anthr)$_2$](Ac)$_2$	-33.33	J_1= -25 J_2= -100	100.34
[oxmglxCu$_3$(his)$_2$](Ac)$_2$	-100	J_1= -44 J_2= -100	99.72
[oxmglxCu$_3$(trp)$_2$](Ac)$_2$	-23.33	J_1= -5.0 J_2= -250	97.77
[oxmglxCu$_3$(tyr)$_2$](Ac)$_2$	-100	J_1= -70 J_2= -250	100.85

Thus, in case of complexes **[oxmglxCu$_3$(anthr)$_2$](Ac)$_2$** and **[oxmglxCu$_3$(his)$_2$](Ac)$_2$**, J_2 values were found to be -100cm^{-1} with the little variation in J_1 as -25 and -44cm^{-1}. In case of complexes **[oxmglxCu$_3$(trp)$_2$](Ac)$_2$** and **[oxmglxCu$_3$(tyr)$_2$](Ac)$_2$** , J_2 values were found to be -250cm^{-1} with a little variation in J_1 as -5 and -70cm^{-1}.

Apparently, the extent of spin exchange between the neighbouring metal centres is not affected by the dihedral angle but is more affected by the electron density and the nature of the terminal ligands. trp and tyr are electron rich and stronger sigma donors as compared to anthranilate and his. The stronger ligand field is probably adjusting the energy of paramagnetic orbital of the terminal copper ion with energy of exchange propagating bridging ligand orbitals, thus resulting in stronger antiferromagnetic exchange as compared to the complexes of anthranilate and histidine. As far as the exchange between the terminal copper ions through the central copper ion and the bridging ligand is concerned, the values of J1 follow the approximate order of the dihedral angle between the copper coordination planes in the complexes of three α-amino acids. In the complexes of trp, his and tyr, the dihedral angle increase from 97.7 to 100.8 and the value of -J also increases in the same order from 5.0 to 70cm^{-1}. Thus it appears that, for the interaction between the neighbouring centres, the coordination geometry and the energy of the paramagnetic orbitals play an important role when a bridging ligand is an efficient mediator of spin exchange. However, the long range interactions are mainly governed by the geometrical parameters.

3.6 Cyclic voltammetric studies

The electrochemical behaviour of all the five trinuclear complexes has been studied by cyclic voltammetry. Two of the typical cyclic voltammograms are shown in **Fig. 3.20** and the potentials are listed in Table 3.8.

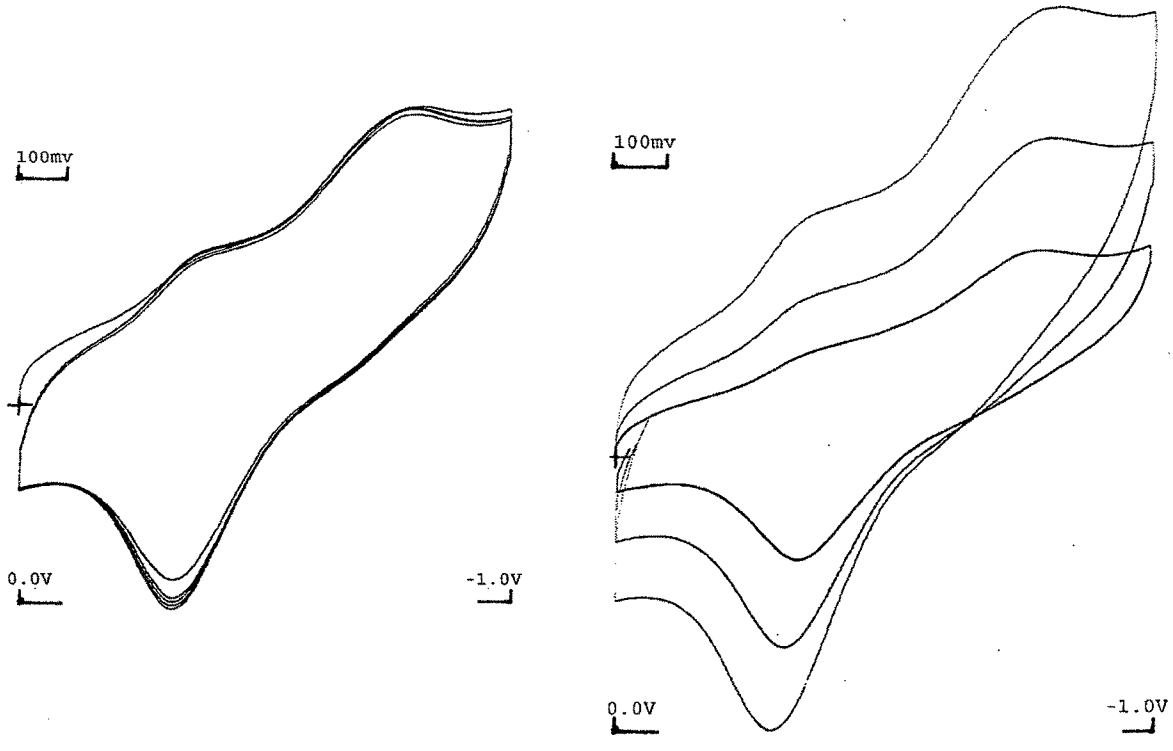

[oxmglxCu$_3$(tyr)$_2$](Ac)$_2$ **[oxmCu$_3$(tyr)$_2$](Ac)$_2$** at 20, 50 & 100mV/s

Pt disk working electrode, Pt wire counter electrodes and Ag/AgNO$_3$ (0.1M in CH$_3$CN) as reference electrodes were used.

Fig.3.20 Cyclic voltammograms of complex **[oxmglxCu$_3$(tyr)$_2$](Ac)$_2$.**

Table 3.8 Redox potentials of the complexes of oxmglx *

Complex	Redox Potentials					
	$Ep_{c(1)}$	$Ep_{c(2)}$	$Ep_{c(3)}$	$Ep_{a(1)}$	$Ep_{a(2)}$	$Ep_{a(3)}$
[oxmglxCu$_3$(anthr)$_2$](Ac)$_2$	-0.353	-0.495	---	-0.320	---	---
[oxmglxCu$_3$(phe)$_2$](Ac)$_2$	-0.370	-0.811	-1.836	-0.311	---	---
[oxmglxCu$_3$(his)$_2$](Ac)$_2$	-0.378	-0.753	-1.378	-0.084	---	---
[oxmglxCu$_3$(trp)$_2$](Ac)$_2$	-0.386	-0.836	-1.911	-0.370	---	-0.745
[oxmglxCu$_3$(tyr)$_2$](Ac)$_2$	-0.403	-0.845	-1.895	-0.370	---	-0.720

*The cyclic voltametric experiment was carried out at Pt electrode in DMSO [0.1MTBAP]. The potentials are referred to Cp_2Fe/Cp_2Fe^+ couple.

Two distinct reduction processes and corresponding oxidation peaks have been observed. In the complexes of amino acids when the voltammograms are recorded between 0.0 to -1.0V region, the complexes undergo first reduction between -0.35 to -0.4V. A second reduction is also observed in all complexes variably between -0.49 to -0.85V. The first reduction is almost reversible in all the complexes. The voltammograms are retraceble indicating reversible redox.

These two reductions can be assigned to stepwise reduction of the three copper(II) centres to copper(I) state. In the complexes **[oxmglxCu$_3$(anthr)$_2$](Ac)$_2$** and **[oxmglxCu$_3$(phe)$_2$](Ac)$_2$** only one corresponding peak is observed. In the complexes of **[oxmglxCu$_3$(trp)$_2$](Ac)$_2$** and **[oxmglxCu$_3$(tyr)$_2$](Ac)$_2$,** corresponding oxidation peaks are observed.

A third reduction is observed in all the complexes without **[oxmglxCu$_3$(anthr)$_2$](Ac)$_2$** complex, between -1.3 to -1.9V (-0.9 to -1.5V v/s NHE). Also the whole redox process becomes electrochemically irreversible in the extended potential region. In the complexes of trp and tyr, the process becomes chemically irreversible too.

The first reduction potential is observed to follow a definite order with the reduction becoming more and more difficult from anthr < phe < his < trp < tyr. This is the approximate order of increasing polarity or decreasing ability of amino acids to delocalize electron density. his, trp and tyr are electron rich with the presence of nitrogen and –OH group as compared to phe while anthr has phenyl ring partly becoming a part of the chelate ring and hence is expected to help the delocalization of added electron more efficiently as compared to the other amino acid. It also appears that there is an effective delocalization of electron density over the metal ions through trinucleating ligands. As a result, addition of subsequent electron becomes difficult and the second reduction occurs at more negative potential.

However, it is not clear if the terminal or central metal ion undergoes first reduction. The central coordination pocket is expected to have more effective π-interaction with the central copper through two imine nitrogens and two amide coordinating sites. This site is expected to undergo easier reduction as compared to

the terminal copper ions. Thus the first reduction can be assigned to central metal ion followed by simultaneous two electron reduction of two terminal copper ions at higher potentials. In the complexes of trp and tyr the oxidation also takes place in steps. This indicates that the delocalization of electron density between the metal ion through the bridging ligand is more in these complexes. Usually, the presence of a non-π-bonding ligand bound to a metal ion increases the π-interaction with a second ligand with π-bonding ability in a ternary species. The trinucleating **oxmglx** is a π-bonding ligand with complete π delocalization. In presence of non-π-bonding tyr and trp with electron rich groups, a π-interaction between the metal ion and the **oxmglx** is expected to be stronger. Strong electron density delocalization has resulted in stepwise reduction as well as oxidation. A more effective electron delocalization in these complexes also indicates a possibility of strong spin delocalization. Thus the exchange coupling in these complexes is expected to be stronger than the complexes of anthr, phe and his. Strikingly the complexes of try and tyr have been found to undergo a very strong antiferromagnetic interaction than the other complexes in this series. The values of coupling constant J_2, being -250cm^{-1} or trp and tyr complexes as compared to -100cm^{-1} in the complexes of anthr and his. Thus, the redox properties and magnetic exchange are related.

REFERENCES

(1) Tsukihara, T., Aoyama, H., Yamashita, E., Tomizaki, T., Yamaguchi, H., Shinzawa-Itoh, K., Nakashima, R., Yonono, R., and Yoshikawa, S. *Science,* 1995, **269,** 1069.

(2) Iwata, S., Ostermeier, C., Ludwig, B., and Michel, H. *Nature,* 1995, **376,** 660.

(3) (a) Yasui, T.; Fujita, J. and Shimura, Y. *This Bulletin,* 1969, **42,** 2081. (b) Fujita, J.; Yasui, T.; and Shimura, Y. *ibid.,* 1965, **38,** 654. (c) Yasui, T.; Hidaka, J. and Shimura, Y. *ibid.,* 1966, **39,** 2417. (d) Hawkins, C. J.; and Lawson, P. J. *Inorg. Chem.,* 1970, **9,** 6. (e) Alexander, M. D. and Busch, D. H. *ibid.,* 1966, **5,** 1590. (f) Fuji, Y. *This Bulletin,* 1972, **45,** 3084. (g) Dellenbaugh, G. G. and Douglas, B. E. *Inorg. Nucl. Chem. Lett.,* 1973,**9,** 1255.

(4) Y. Shimura, *This Bulletin,* 1951, **173,** 315.

(5) (a) Liu, C. T. and Douglas, B. E. *Inorg. Chem.,* 1964, **3,** 1356. (b) Hall, S. K. and Douglas, B. E. *ibid,* 1969, **8,** 372.

(6) Yasui, T. and Douglas, B. E. *ibid,* 1971, **10,** 97.

(7) Matsuoka, N.; Hidaka, J. and Shimura, Y. *This bulletin,*1967, **40,** 1868.; 1972, **45,** 2491.; *Inorg. Chem.,* 1970, **9,** 719.

(8) (a) Nakai, K.; Kanazawa, S. and Shibata, M. *This Bulletin,* 1972, **45,** 3544.; (b) Kojima, Y. and Shibata, M. *Inorg. Chem.,* 1973, **12,** 1009.

(9) Yamada, S.; Hidaka, J. and Douglas, B. E. *Inorg. Chem.,* 1971, **10,** 2187.

(10) Oonishi, I.; Shibata, M.; Marumo, F. and Saito, Y. *Acta Crystallogr, (B),*1973, **29,** 2448.

(11) Bagger, S.; Gibson, K. and Sorensen, C. S. *Acta Chem. Scand.,* 1972, **26,** 2503.

(12) Calabrese, L.; Carbonaro, M. and Musci, G. *The J. of Biological Chemistry,* 1989, **264,** 11, 6183.

(13) Gamez, P.; Aubel, P. G.; Drissen, W. L. and Reedijk, J. *Chem. Soc. Rev.,* 2001, **30,** 376.

(14) (a) Zhang, C. X., Liang, H.-C.; Humphreys, K. J. and Karlin, K. D. in Copper-Dioxygen Complexes and Their Roles in Biomimetic oxidation Reactions, ed. L. Simandi, Dordrecht, The Netherlands, 2001. (b) Than,R.; A. A. and Feldmann, Krebs, B. *Coord. Chem Rev.,* 1999, **182,** 211. (c) Itoh, S. and Fukuzumi, S. *Bull. Chem. Soc. Jpn.,* 2002, **75,** 2081.

(15) (a) Singh, K.; Long, J. R. and Stavropoulos, P. *Inorg. Chem.,* 1998, **37,** 1073. (b) Monzani, E.; Casella, L.; Zoppellaro, G.; Gullotti, M.; Pagliarin, R.; Bonomo, R. P.; Tabbi, G.; Nardin, G. and Randaccio, L. *Inorg. Chim. Acta,* 1998, **282,** 180.

(16) (a) Messerschmidt, A.; Ladenstein, R.; Huber, R.; Bolognesi, M.; Avigliano, L.; Petruzzelli, R.; Rossi, A. and Finazzi-Agro, A. *J. Mol. Biol.,* 1992, **224,** 179. (b) Zaitsev, V. N.; Zaitseva, I.; Papiz, M. and Lindley, P. F. *J. Biol. Inorg. Chem.,* 1999, **4,** 579. (c) Bertrand, T.; Jolivalt, C.; Briozzo, P.; Caminade, E.; Joly, N.; Madzak, C. and Mougin, C. *Biochemistry,* 2002, **41,** 7325. (d) Hakulinen, N.; Kiiskinen, L.-L.; Kruus, K.; Saloheimo, M.; Paananen, A.; Koivula, A. and Rouvinen, J. *Nature Struct. Biol.,* 2002, **9,**601.

(17) (a) Thomas, A. M.; Naik, A. D.; Nethaji, M. and Chakravarty, A. R. *Indian J. Chem.,* 2004, **43A,** 691. (b) Li, Q.; Yang, P.; Wang, H. and Guo, M.; J. *Inorg. Biochem.* 1996, **64,** 181.

(18) Sacht, C.; Datt, M. S.; Otto, S. and Roodt, A. *J. Chem. Soc., Dalton Trans.,* 2000, 727.

(19) Chauhan, M. and Arjmand, F. *Transition Metal Chemistry,* 2005, **30,** 481.

(20) Ferrari, R. P.; Laurenti, E.; Ghibaudi, E. M. and Casella, L. *biochem. Pharmacology, 1997,* **24,** 3868.

(21) Schmidt, M.W.; Baldridge, K. K.; Boatz, J. A.; Elbert, S. T.; Gordon, M. S.; Jensen, J. J.; Koseki, S.; Matsunaga, N.; Nguyen, K. A.; Su, S.; Windus, T. L.; Dupuis, M.; Montgomery, J. A. *J.Comput.Chem.* 1993, **14,** 1347.

(22) Ditchfield, R.; Hehre, W. J.; Pople, J. A.; *J. Chem. Phys.* 1971, **54,** 724.

(23) Hehre, W. J.; Ditchfield, R.; Pople, J. A.; *J. Chem. Phys.* 1972, **56,** 2257.

(24) Rassolov, V. A.; Pople, J. A.; Ratner, M. A.; Windus, T. L.; *J. Chem. Phys.*1998, **109,** 1223.

(25) Rappe', A. K., *et al* JACS, 1992, **114,** 10024.

(26) Casewit, C. J., Colwell, K. S., and Rappe', A. K., *J. Am. Chem. Soc.,* 1992, **114,** 10035.

(27) Casewit, C. J., Colwell, K. S., and Rappe', A. K., *J. Am. Chem. Soc.,* 1992, **114,** 10046.

(28) Rappe', A. K. and Goddard, W. A., *J. Phy. Chem.,* 1991, **95,** 3358.

(29) Rappe', A. K., Colwell, K. S., and Casewit, C. J., *Inorg. Chem.*1993,**32,** 3438.

(30) Thompson, M. A., Zerner M. C. *J. Am. Chem. Soc.,* 1991, **113,** 8210.

(31) Thompson, Mark A.; Glendening, Eric D. and Feller, David *J. Phys. Chem. 1994,* 10465.

(32) Thompson, Mark A. and Schenter, Gregory K. *J. Phys. Chem.* 1995, **99,** 6374.

(33) Thompson, Mark A.; J. Phys. Chem. 1996, **100,** 14492.